Magnetic Interactions and Spiral Ground States in Spinels, with Application to $ZnCr_2Se_4$

K. DWIGHT AND N. MENYUK

Lincoln Laboratory, Massachusetts Institute of Technology, Lexington, Massachusetts*

(Received 6 June 1967)

It is found that five distinct distant-neighbor interactions must be considered in order to characterize adequately the Heisenberg energy in normal cubic spinels having diamagnetic A-site ions. The classical theory of the ground spin state is presented in terms of these interactions, which span a five-dimensional parameter space. It is demonstrated that the ground state consists of a spiral spin configuration with $\mathbf{k}=(0,0,l)$ if and only if the parameter values fall inside a limited region, which is determined rigorously by means of the Luttinger-Tisza method. Because of the circumscription of this spiral ground-state region, agreement with the experimental findings for $ZnCr_2Se_4$ requires that at least one of the distant-neighbor interactions be ferromagnetic. Furthermore, these interactions can be analyzed into their constituent superexchange terms, which can in turn be related by standard superexchange theory. The resulting criteria for physical reasonability place additional limits upon the acceptable range of values for the interactions. This range is found to exclude those sets of interactions which have previously been proposed in the literature. A simplified superexchange model is used to illustrate the determination of physically reasonable fits to the data and to study their dependence upon the degree of A-site covalence.

I. INTRODUCTION

EXPERIMENTAL studies of zinc selenio-chromite have been made by several workers. Lotgering found $ZnCr_2Se_4$ to be an antiferromagnetic cubic spinel with a positive asymptotic Curie temperature of 115°K,[1] Allain found that its spins could be realigned ferromagnetically at 4.2°K by the application of an external field of 64 kOe,[2] and Plumier found its ground spin state to be a $(0, 0, l)$ spiral with a turn angle of 42°.[3] Lotgering was able to account for his findings on the basis of a strongly ferromagnetic nearest-neighbor Cr-anion-Cr interaction, together with relatively weak, antiferromagnetic second-, third-, and fourth-nearest-neighbor exchange couplings through two anions. Plumier considered only three interactions and, therefore, was able to evaluate them uniquely from the above data. According to his calculations based on these assumptions, the first- and second-nearest-neighbor interactions are both ferromagnetic and only that between third-nearest-neighbors is antiferromagnetic.

However, zinc selenio-chromite is not an isolated material; several other chromium chalcogenide spinels having diamagnetic A-site cations have also been investigated. Some of these are ferromagnetic, such as $CdCr_2Se_4$.[4,5] It has been pointed out that the marked dependence upon the A ion indicated by comparison of the properties of zinc and cadmium homologues does not require the A site to be directly responsible for the exchange mechanism.[5] However, the theory for the ferromagnetic materials recently developed by Baltzer, Wojtowicz, Robbins, and Lopatin is based upon the presupposition that distant-neighbor interactions occur exclusively via the A ions, and hence must all be antiferromagnetic.[6] They rejected Plumier's findings (which contradict their model), but their grounds for this rejection are shown to be in error in Sec. IV of this paper.

Nevertheless, the restriction of Plumier's analysis to three interactions does leave room for equivocation. We find that an adequate characterization of the Heisenberg energy requires the consideration of five distinct more-distant-neighbor interactions. Each of these interactions is analyzed in terms of their constituent superexchange terms[7,8] in Sec. II. This decomposition also serves to clarify the possible effects of covalency.

In order to reach more definitive conclusions about the interactions in such materials, we have investigated theoretically the ground spin states of normal cubic spinels with diamagnetic A ions. The mathematical treatment outlined in Sec. III employs the method of Luttinger and Tisza[9] to delineate rigorously both the ferromagnetic and the spiral ground-state regions in a five-dimensional exchange-parameter space. In Sec. IV, two relations among the five exchange ratios are obtained from the experimental results for $ZnCr_2Se_4$. This step suffices to prove that at least one of the more-distant-neighbor interactions must be ferromagnetic, no thermodynamic approximations being involved.

* Operated with support from the U.S. Air Force.

[1] F. K. Lotgering, in *Proceedings of the International Conference on Magnetism, Nottingham, 1964* (The Institute of Physics and The Physical Society, London, 1965), p. 533.

[2] Y. Allain, F. Varret, and A. Miedan-Gros, Compt. Rend. **260**, 4677 (1965).

[3] R. J. Plumier, Compt. Rend. **260**, 3348 (1965); J. Phys. (Paris) **27**, 213 (1966).

[4] P. K. Baltzer, H. W. Lehmann, and M. Robbins, Phys. Rev. Letters **15**, 493 (1965).

[5] N. Menyuk, K. Dwight, R. J. Arnott, and A. Wold, J. Appl. Phys. **37**, 1387 (1966).

[6] P. K. Baltzer, P. J. Wojtowicz, M. Robbins, and E. Lopatin, Phys. Rev. **151**, 367 (1966).

[7] P. W. Anderson, Phys. Rev. **115**, 2 (1959).

[8] J. B. Goodenough, *Magnetism and the Chemical Bond* (Interscience Publishers Inc., New York, 1963), pp. 165–184.

[9] J. M. Luttinger and L. Tisza, Phys. Rev. **70**, 954 (1946); **81**, 1015 (1951).

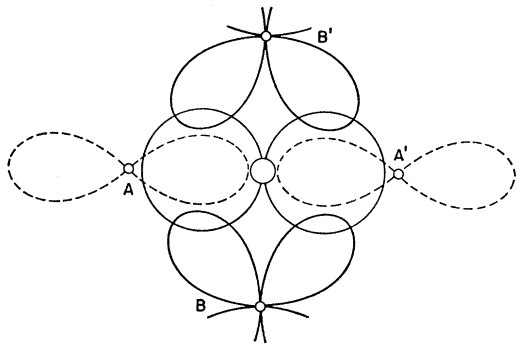

FIG. 1. Types of nearest-neighbor superexchange through an intermediary anion.

Although Plumier's values constitute a mathematically valid solution, they are shown to be physically unreasonable in Sec. V by the application of the standard rules of superexchange.[10,11] Finally, a simple model is advanced both to illustrate the procedure for obtaining physically consistent solutions to the mathematical problem and to investigate the effects of covalency. It is thereby shown that the heretofore neglected interaction is important, that the deduced values for the exchange interactions are rather insensitive to the internal parameters of the model, and that the permissible covalent effect is limited.

II. ANALYSIS OF EXCHANGE INTERACTIONS

Consider a normal, cubic spinel whose A sites are occupied by nonmagnetic ions. The classical Heisenberg energy is given by

$$E=-\sum_{n\nu,m\mu}\bar{J}_{n\nu,m\mu}\mathbf{S}_{n\nu}\cdot\mathbf{S}_{m\mu}$$
$$=-\bar{J}\sum_{n\nu,m\mu}\mathcal{J}_{n\nu,m\mu}\mathbf{S}_{n\nu}\cdot\mathbf{S}_{m\mu}, \quad (1)$$

where $\mathbf{S}_{n\nu}$ is a unit vector in the direction of the spin on the $n\nu$th site, n and m run over the unit cells in the sample, ν and μ run over the four crystallographically different B sites within a unit cell, the $\bar{J}_{n\nu,m\mu}$ are the exchange constants (positive when ferromagnetic) multiplied by the magnitudes of the spins, and the $\mathcal{J}_{n\nu,m\mu}$ are the ratios of these interactions to the dominant nearest-neighbor interaction $\bar{J}$. In the insulating materials under consideration, these interactions arise from various superexchange linkages connecting pairs of $3d$ orbitals. Each superexchange linkage consists of a sequence of overlapping ionic orbitals, starting from a $3d$ orbital at the $n\nu$th site and ending with a $3d$ orbital at the $m\mu$th site, and makes a contribution (of the order of the product of all the overlap integrals encountered) to the transfer integral connecting those two particular orbitals.[7,8] In turn, each interacting pair of orbitals contributes to the exchange $\bar{J}_{n\nu,m\mu}$ an energy proportional to the square of its transfer integral, multiplied by factors dependent on ionization energies, electron configurations, etc.[7,8] The usual classification of the resulting $\bar{J}_{n\nu,m\mu}$ into second-nearest neighbor, third-nearest neighbor, etc., based upon the separation between interacting cations yields little insight into their relative strengths, and can even be misleading. Rather, a detailed examination of the individual superexchange terms contributing to each $\bar{J}_{n\nu,m\mu}$ is required for the determination of a physically reasonable set of exchange parameters $\mathcal{J}_{n\nu,m\mu}$.

The crystal-field splitting of the $3d$ manifold gives rise to two varieties of overlap of a cation $3d$ wave function with a given anion p orbital, as illustrated schematically in Fig. 1. The e_g orbitals of cations A and A' each overlap the p orbital along its axis, forming so-called σ bonds. The off-axis overlaps of the t_{2g} orbitals of cations B and B' with the anion p form π bonds. A pair of such bonds is involved in each nearest-neighbor superexchange linkage, which can therefore be of three types: σ-σ, as between A and A'; π-π, as between B and B'; and σ-π, as between A and B'. If σ and π represent overlap integrals, then the respective transfer integrals will vary as σ^2, π^2, and $\sigma\pi$, and the resulting exchange constants as σ^4, π^4, and $(\sigma\pi)^2$, apart from other factors.

The case of more distant neighbors is illustrated in Fig. 2. Again there are three types of coupling: σ-Δ-σ, as between A and A''; π-Δ-π, as between B and B''; and σ-Δ-π as between A and B''. These linkages involve the same σ and π cation-anion overlaps as before—the only change is the addition of an anion-anion overlap, denoted by Δ. This additional factor of Δ in the transfer integral multiplies the exchange by Δ^2, and results in a uniform reduction which leaves the signs and relative strengths of these interactions unchanged from those of their nearest-neighbor counterparts.

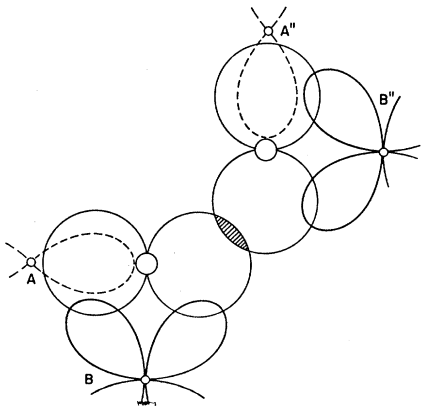

FIG. 2. Types of more-distant-neighbor superexchange through two intermediary anions.

[10] J. B. Goodenough, J. Phys. Chem. Solids **6**, 287 (1958).
[11] J. Kanamori, J. Phys. Chem. Solids **10**, 87 (1959).

Now consider the spinel structure, a portion of which is shown in Fig. 3. Here the four different B sublattices are denoted by subscripts, and some of the anions are numbered for the purpose of identification. Within a particular face-centered B sublattice, say that with $\mu=3$, a given site (such as B_3 in Fig. 3) has twelve nearest neighbors which are subdivided into two groups of six. B_3'' shares a chain of B sites with B_3 and typifies one group; B_3' illustrates the other group. The pair B_3-B_3'' is separated by a vector $\tau_{n\mu}{}^{m\mu}$, which belongs to the (2, 2, 0) family; the pair B_3-B_3' by one belonging to the $(2, \bar{2}, 0)$ family. We define $\bar{J}(B_3\text{-}B_3'')\equiv\bar{J}(2, 2, 0)$ and $\bar{J}(B_3\text{-}B_3')\equiv\bar{J}(2, \bar{2}, 0)$. As detailed in Appendix A, these exchange constants contain several superexchange terms, some of which involve multiple paths (linkages). When the dominant anion-anion overlap Δ is sufficiently large compared with the lesser overlaps included in the results of Appendix A, one obtains, from Eqs. (A1) and (A2),

$$\bar{J}(2, 2, 0)\equiv U\bar{J}\cong\sum_{i,j}\{\sigma_i[2\Delta]\sigma_j\}+\{\pi[2\Delta_B]\pi\}, \quad (2)$$

$$\bar{J}(2, \bar{2}, 0)\equiv U'\bar{J}\cong\sum_{i,j}\{\sigma_i[2\Delta_A]\sigma_j\}+\{\pi[2\Delta_A]\pi\}. \quad (3)$$

Here the curly brackets represent distinct superexchange terms connecting different pairs of cation orbitals and enclose products of orbital overlaps which behave like the corresponding transfer integrals. The subscripts A and B indicate overlaps which may be augmented (or diminished, depending on phases) by covalency with A- or B-site cations, respectively. The parameters U and U' will be equal when there is no covalency effect.

Other interactions involve sites lying in different sublattices. The ions B_3 and B_4' in Fig. 3, for example, are separated by a vector $\tau_{n\nu}{}^{m\mu}$, which belongs to the (3, 1, 0) family; the pair B_3-B_1' by one belonging to the (2, 1, 1) family. With the definitions $\bar{J}(B_3\text{-}B_4')\equiv\bar{J}(3, 1, 0)$ and $\bar{J}(B_3\text{-}B_1')\equiv\bar{J}(2, 1, 1)$, Eqs. (A3) and (A4) yield

$$\bar{J}(3, 1, 0)\equiv V\bar{J}\cong 2\sum_i\{\sigma_i[2\Delta_A]\pi\}, \quad (4)$$

$$\bar{J}(2, 1, 1)\equiv W\bar{J}\cong 2\sum_i\{\sigma_i[\Delta+\Delta_A]\pi\}+\{\pi[\Delta+2\Delta_A]\pi\}+\{\pi[3\Delta_B]\pi\}, \quad (5)$$

when Δ is sufficiently dominant. Still other interactions involve even more distant neighbors, such as B_3 and B_3'''. With $\bar{J}(B_3-B_3''')\equiv\bar{J}(4, 0, 0)$, it follows from Eq. (A5) that

$$\bar{J}(4, 0, 0)\equiv U_2\bar{J}\cong\sum_{i,j}\{\sigma_i[4\Delta_A\Delta]\sigma_j\}+2\{\pi[2\Delta_A\Delta_B]\pi\}, \quad (6)$$

which need not be negligible. We shall include this interaction in our calculations to obtain an estimate of the potential importance of such terms depending upon two anion-anion overlaps, of which there are several others.

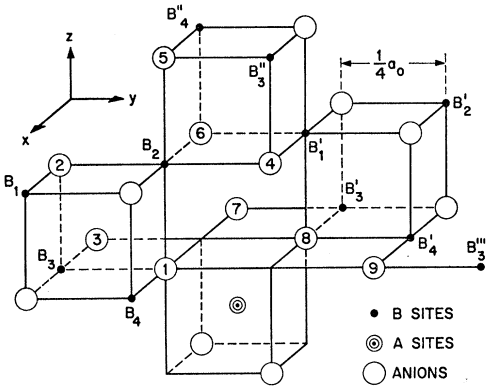

FIG. 3. Positions of the anions and cations in the spinel structure.

In Table I the exchange parameters U, U', V, W, and U_2 defined above are compared with other notations which have appeared in the literature. These parameters will be treated as arbitrary mathematical variables in the next two sections of this paper. However, in Sec. V we shall return to the concept of superexchange to discuss the inference of the signs and relative strengths of the interactions for the particular case of trivalent chromium (empty e_g and half-filled t_{2g} orbitals).

III. GROUND-STATE CALCULATIONS

It is convenient to work with the Fourier transform of Eq. (1)[12–14]:

$$E=-N\bar{J}\sum_{\mathbf{k}}\sum_{\nu\mu}L_{\nu\mu}(\mathbf{k})\,\mathbf{Q}_\nu{}^*(\mathbf{k})\cdot\mathbf{Q}_\mu(\mathbf{k}), \quad (7)$$

where

$$\mathbf{S}_{n\nu}=\sum_{\mathbf{k}}\mathbf{Q}_\nu(\mathbf{k})\exp(i\mathbf{k}\cdot\mathbf{R}_{n\nu}), \quad (8)$$

$$L_{\nu\mu}(\mathbf{k})=\sum_m\mathcal{J}_{n\nu,m\mu}\exp(i\mathbf{k}\cdot\tau_{n\nu}{}^{m\mu}), \quad (9)$$

with $\tau_{n\nu}{}^{m\mu}=\mathbf{R}_{m\mu}-\mathbf{R}_{n\nu}$. We shall use the notation $\mathbf{R}=(a_0/4)(r, s, t)$ for vectors in real space, and $\mathbf{k}=(2\pi/a_0)(h, k, l)$ for vectors in reciprocal space, a_0 being the usual cell edge. In addition, $\mathbf{R}_{n\nu}=\mathbf{R}_n+\varrho_\nu$, where the lattice vector $\mathbf{R}_n$ is expressed in terms of the basic face-centered translations (2, 2, 0), (2, 0, 2), and (0, 2, 2), and where the four B sites in the unit cell occupy the positions $\varrho_\nu=(1, 0, 1)$, (0, 1, 1), (0, 0, 0), and (1, 1, 0) as ν runs from 1 to 4. The matrix elements $L_{\nu\mu}(\mathbf{k})$ are given explicitly in Appendix B as functions of the five exchange ratios introduced in Sec. II.

Minimization of the energy is equivalent to maximization of the summation over $\mathbf{k}$ in Eq. (7) when $\bar{J}$ is ferromagnetic (>0), as in $ZnCr_2Se_4$. We wish to demon-

[12] D. H. Lyons and T. A. Kaplan, Phys. Rev. **120**, 1580 (1960).
[13] D. H. Lyons, T. A. Kaplan, K. Dwight, and N. Menyuk, Phys. Rev. **126**, 540 (1962).
[14] N. Menyuk, K. Dwight, D. Lyons, and T. A. Kaplan, Phys. Rev. **127**, 1983 (1962).

TABLE I. Notations used for the various interactions considered by different investigators.

Interaction	Present	L[a]	P[b]	BWRL[c]
$J(1,1,0)$	J	W_0	W_0	J
$J(2,2,0)$	UJ	W_2	W_2	...
$J(2,\bar{2},0$	$U'J$	W_3	W_2	K
$J(3,1,0)$	VJ	W_4	...	K
$J(2,1,1)$	WJ	W_1	W_1	K
$J(4,0,0)$	U_2J	...	...	...

[a] Reference 1.
[b] Reference 3.
[c] Reference 6.

strate spin configurations (sets of unit vectors $\mathbf{S}_{n\nu}$) which achieve this goal for various values of the exchange parameters. Our procedure has been described in detail elsewhere.[12–14] In essence, the Luttinger-Tisza argument proves that a spin configuration is rigorously the ground state whenever it is represented by the eigenvector associated with the maximum eigenvalue (over all $\mathbf{k}$) of the matrix function $\mathbf{L}(\mathbf{k})$.[9,12] Conversely, it can be shown that a planar spin configuration rigorously cannot be the ground state whenever it is not represented by the maximum eigenvector of $\mathbf{L}(\mathbf{k})$.[15] Thus, representation by the maximum eigenvector constitutes the necessary and sufficient condition for a planar configuration to be the ground state.

Consider the case where $\mathbf{k}=(2\pi/a_0)(0, 0, l)$. It follows from Appendix B, abbreviating $L_{\nu\mu}(0, 0, l)$ as $L_{\nu\mu}(l)$, that

$$L_{\mu\mu}(l)=(2U+2U'+4U_2)+(4U+4U')\cos(2l')+2U_2\cos(4l') \quad (10)$$

for all μ, with $l'=\frac{1}{2}(\pi l)$, and

$$L_{12}(l)=L_{34}(l)=(2+4V)+4W\cos(2l'), \quad (11)$$

$$L_{\nu\mu}(l)=(2+2V+4W)\cos(l')+2V\cos(3l'), \quad (12)$$

for all other $\nu<\mu$, and of course $L\nu\mu(l)=L_{\mu\nu}(l)$. The eigenvectors $\psi_\alpha(l)$ of this matrix are $(1/2)(1, 1, 1, 1)$, $(1/2)(1, -1, 1, -1)$, $(1/2)(1, -1, -1, 1)$, and $(1/2)(1, 1, -1, -1)$ as α runs from 1 to 4. These eigenvectors all represent planar spin configurations, and their eigenvalues $\lambda_\alpha(l)$ can be written as

$$\lambda_1(l)=2(1-U-U'+2V-2W+3U_2)+4(1-2V+2W)\cos l'+8(U+U'+W-2U_2)\cos^2 l'+16V\cos^3 l'+16U_2\cos^4 l', \quad (13)$$

$$\lambda_2(l)=\lambda_3(l)=2(-1-U-U'-2V+2W+3U_2)+8(U+U'-W-2U_2)\cos^2 l'+16U_2\cos^4 l', \quad (14)$$

$$\lambda_4(l)=\lambda_1(2-l). \quad (15)$$

[15] This theorem is proved in footnote 15 of Ref. 13.

Since these equations involve only the sum of U and U', it is convenient to introduce the new variables $\bar{U}$ and γ such that

$$U=\bar{U}(1-\gamma) \quad \text{and} \quad U'=\bar{U}(1+\gamma). \quad (16)$$

We have determined the maximum $\lambda_\alpha(l)$ throughout the five-dimensional parameter space being investigated. Some of our findings are illustrated in Fig. 4, which shows a portion of the $\gamma=W=U_2=0$ plane. The ferromagnetic state $\lambda_1(0)$ lies highest when all the parameters are positive (all interactions ferromagnetic). However, the collinear antiferromagnetic state $\lambda_2(0)$ overtakes it when $V<-0.5$, and the spiral state $\lambda_1(l)$ overtakes it when $\bar{U}$ is sufficiently negative. The value of l varies along the $\lambda_1(l)-\lambda_1(0)$ boundary shown in Fig. 4; $l=0$ from C to B, $0<l<1$ from B to A, and $1<l<2$ from A to infinity. The dashed, constant-l lines to the left of this boundary indicate the manner of variation of l within the spiral region. In between the $\lambda_1(l)$ and $\lambda_2(0)$ states, there exists a region where a $\lambda(\frac{1}{2}, \frac{1}{2}, \frac{1}{2})$ lies highest. Its associated eigenvector $\psi=(1/\sqrt{3})(1, 1, 0, 1)$ is related to the configuration observed in $GeNi_2O_4$.[16]

By using an SDS 930 computer, we have established that the above are indeed the maximum eigenvalues of $\mathbf{L}(\mathbf{k})$ over all $\mathbf{k}$ and α inside the regions assigned them in Fig. 4. This result proves the spiral, ferromagnetic, and collinear antiferromagnetic configurations to be the ground states within their respective regions. [The $\lambda(\frac{1}{2}, \frac{1}{2}, \frac{1}{2})$ state poses problems similar to those treated elsewhere,[13] and will not be discussed further in this paper.] However, the all-k computations introduced a "no man's land" between the $\lambda_1(l)$ and $\lambda(\frac{1}{2}, \frac{1}{2}, \frac{1}{2})$ regions, where neither is the maximum eigenvalue.

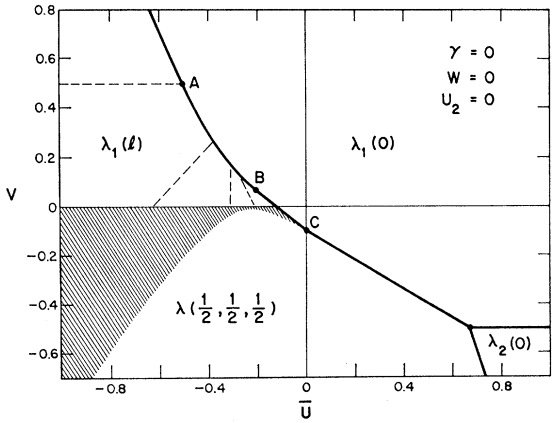

FIG. 4. A slice through exchange-parameter space showing the regions wherein the indicated $\lambda_\alpha(\mathbf{k})$ are the maximum eigenvalues of $\mathbf{L}(\mathbf{k})$ over all α and $\mathbf{k}$. None of these eigenvalues is the maximum inside the shaded region. The dashed lines in the $\lambda_1(l)$ spiral region denote curves of constant $\mathbf{k}=(0,0,l)$.

[16] E. F. Bertaut, Vu Van Qui, R. Pauthenet, and A. Murasik, J. Phys. (Paris) 25, 516 (1964).

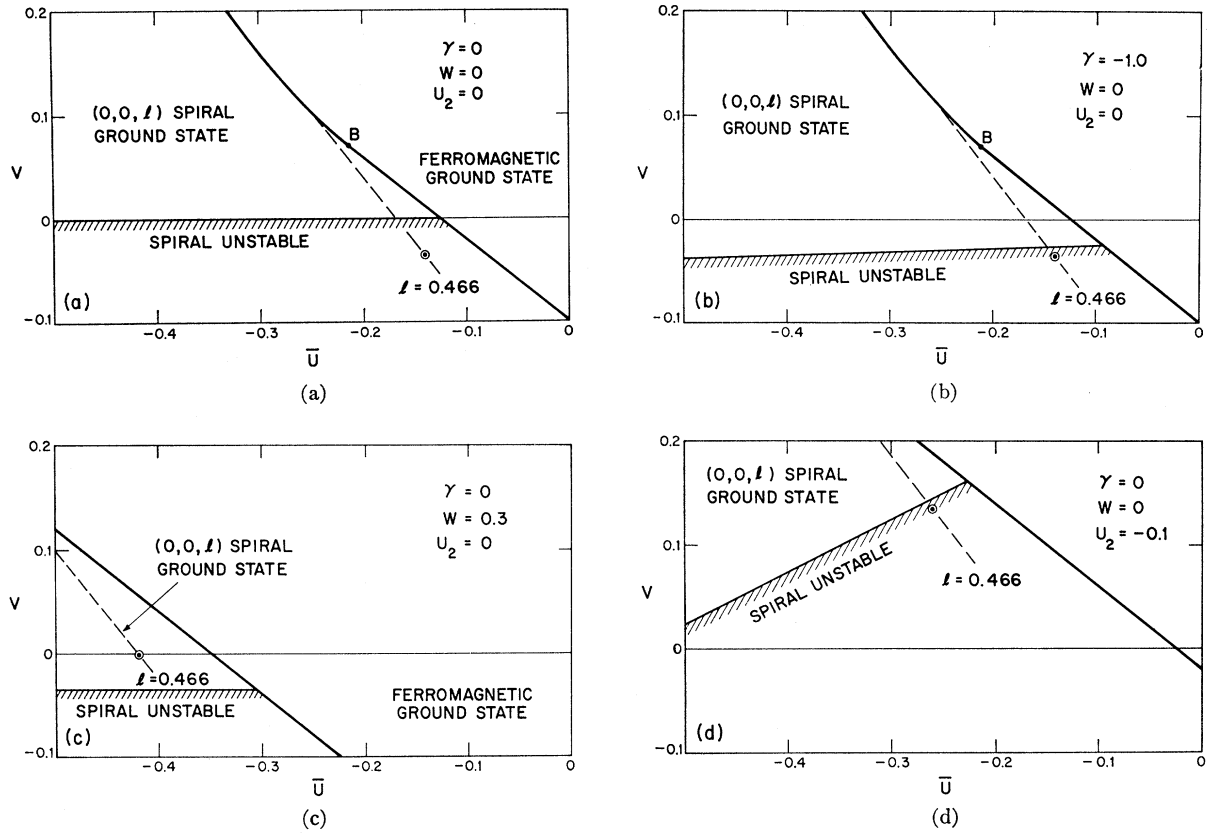

FIG. 5. Slices through exchange-parameter space selected to provide insight into the influence of all the variables upon the spiral instability boundary in the neighborhood of the ferromagnet-spiral border. The circled points represent values of the parameters which fit the experimental data for zinc selenio-chromite, i.e., which satisfy Eq. (25). The dashed lines are the loci of all parameter values corresponding to a spiral configuration with a turn angle of 42°, and the distance of the circled points from the ferromagnetic border is related to the magnetic field required to realign the spins.

The (0, 0, l) spiral state rigorously cannot be the ground state within this instability region, which is shown shaded in Fig. 4. The location of this instability boundary plays an essential role in our interpretation of the experimental results for $ZnCr_2Se_4$.

Consider a spiral spin configuration with some particular value of $l=l_0$ and some particular degree of stabilization δ over the ferromagnetic state, $\delta_0=\lambda_1(l_0)-\lambda_1(0)$. It will be represented by a point in the $\gamma=W=U_2=0$ plane. Such a point, representing the configuration observed in $ZnCr_2Se_4$,[3] is indicated in Fig. 5(a). It lies outside the spiral ground-state region. Consequently this spiral configuration could not be the ground state for that choice of γ, W, and U_2. Negative values of γ tend to stabilize the spiral state, but even $\gamma=-1$ is insufficient for this particular spiral to be the ground state, as shown in Fig. 5(b). Positive values of W also favor the spiral state, but must be compensated by more negative values of $\bar{U}$. Figure 5(c) shows that $W=0.3$ is more than enough to stabilize the spiral.

TABLE II. Stable solutions of Eq. (25) for the simplified model.

δ/Δ	α	$\bar{U}$	γ	V	W	U_2	$\bar{J}/k$ (°K)
0.3	3.3	−0.314	0.245	0.081	0.106	−0.059	25.1
0.2	3	−0.299	0.174	0.081	0.089	−0.060	25.3
0.2	4	−0.305	0.175	0.066	0.109	−0.050	25.0
0.0	3	−0.262	0	0.061	0.061	−0.051	25.7
0.0	6	−0.266	0	0.035	0.088	−0.034	25.3
−0.2	4	−0.235	−0.232	0.032	0.054	−0.034	25.8
−0.2	7	−0.225	−0.228	0.017	0.056	−0.026	25.7
−0.25	4	−0.219	−0.302	0.025	0.042	−0.032	25.6
−0.25	6	−0.219	−0.297	0.016	0.050	−0.026	25.8
−0.29	5	−0.211	−0.358	0.015	0.040	−0.026	25.6

Negative values of U_2 result in more positive V, as illustrated in Fig. 5(d). However, $U_2=-0.1$ is not enough to stabilize this particular spiral when $W=0$.

IV. APPLICATION TO $ZnCr_2Se_4$

Zinc selenio-chromite is a normal, cubic spinel with nonmagnetic Zn^{2+} ions occupying the A sites. It becomes antiferromagnetic below about 20°K, and neutron diffraction has shown its ground state to be a $\mathbf{k}=(0, 0, l_0)$ planar spiral with a turn angle of $l_0'=42°$.[3] However, experiments in pulsed magnetic fields at 4.2°K show that the spins can be realigned ferromagnetically by the application of an external field as small as $H_0=64$ kOe.[2] In addition, susceptibility measurements at higher temperatures show the asymptotic Curie temperature to be $\theta=115$°K.[1] Because of this positive value of θ, the nearest-neighbor exchange interaction $\bar{J}$ can be presumed to be ferromagnetic. Consequently the theoretical treatment of Sec. III is applicable and can be used to deduce relationships among the exchange interactions from the experimental values for l_0, H_0, and θ. The interpretation of these quantities does not involve any approximate statistical mechanics. Furthermore, we consider the slight tetragonal distortion (c/a=0.999) which occurs below T_N[3] to be a secondary effect that, if taken into account, would not materially affect our conclusions.

In our notation, the usual derivation gives

$$k\theta=\tfrac{2}{3}S(S+1)(\bar{J}/S^2)\sum_{m\mu}\mathcal{J}_{n\nu,m\mu}$$
$$=4S(S+1)(\bar{J}/S^2)(1+2\bar{U}+2V+2W+U_2), \quad (17)$$

where S is the B-site spin quantum number and $\bar{J}$ is the nearest-neighbor exchange interaction multiplied by S^2. Furthermore, in the presence of an external magnetic field H, Eq. (7) becomes

$$E/N=-g\mu_B S\mathbf{H}\cdot\sum_{\mu}\mathbf{Q}_{\mu 1}(0)$$
$$-\bar{J}\sum_{\mathbf{k}}\sum_{\nu\mu}L_{\nu\mu}(\mathbf{k})\mathbf{Q}_{\nu}^{*}(\mathbf{k})\cdot\mathbf{Q}_{\mu}(\mathbf{k})$$
$$=-g\mu_B S\mathbf{H}\cdot\sum_{\mu}\mathbf{Q}_{\mu 1}(0)$$
$$-\bar{J}\sum_{\mathbf{k},\alpha}\lambda_{\alpha}(\mathbf{k})\sum_{\mu}|\,\mathbf{Q}_{\mu\alpha}(\mathbf{k})\,|^2, \quad (18)$$

$\mathbf{Q}_{\mu\alpha}(\mathbf{k})$ being proportional to the μth component of the eigenvector $\psi_{\alpha}(\mathbf{k})$. For a conical configuration, $\mathbf{Q}_{\mu 1}(0)=\hat{z}\cos\phi$ and $\mathbf{Q}_{\mu 1}(\pm\mathbf{k}_0)=\frac{1}{2}(\hat{x}\mp i\hat{y})\sin\phi$, so that

$$E/N=-4g\mu_B SH\cos\phi-4\bar{J}[\lambda_1(0)\cos^2\phi+\lambda_1(l_0)\sin^2\phi], \quad (19)$$

where ϕ is the cone angle. Minimization of Eq. (19) yields ϕ as a function of H, and this equilibrium ϕ vanishes when the field strength reaches H_0. The nearest-neighbor interaction $\bar{J}$ can be eliminated by using Eq. (17). Thus

$$\lambda_1(l)-\lambda_1(0)=(g\mu_B SH_0)/(2\bar{J})$$
$$=\left[\frac{2g\mu_B(S+1)H_0}{k\theta}\right](1+2\bar{U}+2V+2W+U_2), \quad (20)$$

where the value of the bracket is 0.374 for zinc selenio-chromite ($gS=3$). But, from Eqs. (13) and (16),

$$\lambda_1(l)-\lambda_1(0)=4(c-1)[1+4\bar{U}(1+c)+2V(1+2c+2c^2)$$
$$+2W(2+c)+4U_2(c^2+c^3)], \quad (21)$$

where we have written c for $\cos l'$. Equations (20) and (21) can be combined to yield the relation (for $ZnCr_2Se_4$)

$$0=1.401+7.912\bar{U}+8.128V+6.385W+4.331U_2. \quad (22)$$

The spiral turn angle l' must maximize Eq. (13). Upon factoring out 4 $\sin l'$, this stationary condition becomes

$$0=1+8\bar{U}c-2V(1-6c^2)+2W(1+2c)-8U_2(c-2c^3), \quad (23)$$

which is the equation of a constant-l surface. When $l'=42°$,

$$0=1+5.945\bar{U}+4.626V+4.972W+0.618U_2. \quad (24)$$

This equation yields the $l=0.466$ surface illustrated by the dashed lines in Figs. 5(a)–5(d). The actual exchange parameters in zinc selenio-chromite must satisfy both Eq. (22) and Eq. (24), so that one obtains the solution

$$\bar{U}=-0.140-0.928W+1.28U_2,$$
$$V=-0.036+0.118W-1.78U_2. \quad (25)$$

These equations yield a point independent of γ in every γ-W-U_2 plane—the circled points in Figs. 5(a)–5(d), for example.

Each such point represents a possible set of values (within experimental error) for the exchange param-

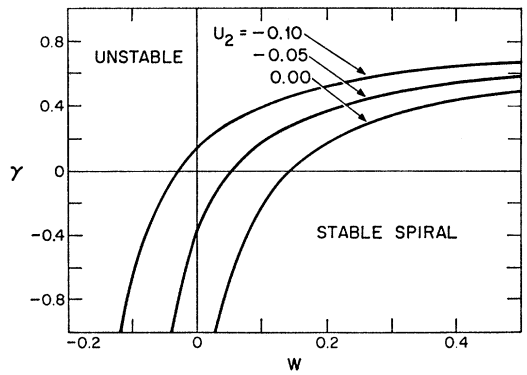

FIG. 6. Values of γ versus W needed to stabilize the spiral ground state of zinc selenio-chromite as represented by solutions of Eq. (25) for particular values of the exchange parameter U_2.

eters in zinc selenio-chromite provided, of course, that it lies inside the spiral ground-state region. Figures 5(a)–5(d) illustrate how this region is limited by the all-k instability boundary in the vicinity of the points in question. Among the planes depicted, only $\gamma=0$, $W=0.3$, $U_2=0$ [Fig. 5(c)] yields a spiral ground state for $ZnCr_2Se_4$, for which $\bar{U}=-0.419$ and $V=-0.001$. This point essentially corresponds to Plumier's solution.[3] More generally, our all-k calculations yield the boundaries shown in Fig. 6 when $\bar{U}$ and V are given by Eq. (25). Positive values for W and negative for γ serve to stabilize the experimentally determined spiral ground state.

Baltzer *et al.*[6] have suggested that Plumier's conclusions are invalidated by his use of molecular-field theory. However, the molecular-field expression for θ is known from the high-temperature susceptibility expansion to be rigorously correct. Furthermore, the determination of a particular $(0, 0, l_0)$ spiral is also reliable, since the classical ground-state spin configuration not only determines the quantization axes in the quantum-mechanical internal-field theory, but also provides the basis for all spin-wave calculations. Finally, spin-wave analysis of collinear antiferromagnets indicates that the classical molecular-field expression for H_0 is accurate when anisotropy is weak,[17] as indeed it is in chromium spinels.[3,18,19] Thus the molecular-field interpretations of these quantities (θ, l_0, and H_0) do not constitute valid grounds for rejecting Plumier's analysis, nor our own.

In our notation, the model proposed by Baltzer *et al.*[6] for chalcogenide spinels requires that $V=W=2\bar{U}$ and $\gamma=1$, with $U_2=0$. However, Eq. (25) possesses no solutions which satisfy these restrictions. In addition, our all-k calculations show all $(0, 0, l)$ spiral configurations to be unstable under these conditions. Even if the restriction of equality among V, W, and $2\bar{U}$ were dropped, there could be no stable solution of Eq. (25) as long as they all remained negative (antiferromagnetic). Thus rigorous consequences of their model contradict experiment, which indicates that its underlying assumptions are unrealistic. Their presupposition that the A ion is solely responsible for distant-neighbor interaction is particularly questionable.

V. INTERPRETATION AND CONCLUSIONS

We have shown that the values for $\bar{U}$ and V computed from Eq. (25) yield agreement with experimental findings for zinc selenio-chromite if and only if the values for the three other exchange parameters γ, W, and U_2 are represented by a point inside the region of spiral stability shown in Fig. 6. This result, obtained by treating the exchange parameters as arbitrary mathematical variables, constitutes a severe limitation on the range of allowed values for these parameters. Further restrictions can be inferred from the physical nature of the interactions by considering their decomposition into the superexchange terms described in Sec. II and detailed in Appendix A.

The signs of the contributions from the various terms can be obtained from the Goodenough-Kanamori rules of superexchange,[10,11] which state that superexchange between two empty or two half-filled orbitals will be negative (antiferromagnetic), whereas that between one empty and another half-filled orbital will be positive. In the particular case of trivalent chromium in octahedral coordination (as on a spinel B site), the e_g orbitals involved in the σ bonds are empty while the t_{2g} orbitals involved in the π bonds are half-filled. Consequently all contributions from $\sigma-\Delta-\sigma$ and $\pi-\Delta-\pi$ linkages will be negative; those from $\sigma-\Delta-\pi$ linkages will be positive. In addition, since π overlaps are smaller than σ overlaps, there can be a tendency for superexchange interactions via π bonds to be weaker than those via σ bonds, even when the latter orbitals are empty. Accordingly, we anticipate the σ-Δ-σ interaction to be the strongest of the three, the π-Δ-π the weakest.

From the above properties of trivalent chromium and the analysis given in Sec. II, where the lesser anion-anion overlaps were neglected, it follows that the interactions U, U', and U_2 are all negative, that V is positive, and that the sign of W is uncertain. It is clearly unrealistic to equate V with U'.[6] It is also unrealistic to speak of a $W=0.3$ when $V=0$.[3] Furthermore, since the superexchange contributions vary as the square of the transfer integral, which in turn behaves like the product of the orbital overlaps,[7] Eqs. (4) and (5) require that $W<(1+\Delta/\Delta_A)^2V$. Only when $U_2<-0.02$ can solutions of Eq. (25) be found which both satisfy this inequality and lie in the stability region of Fig. 6. Thus the neglect of U_2 would preclude any possibility of obtaining physically reasonable agreement with experiment.

The inference of more specific consequences requires that the number of independent variables be reduced, but not by arbitrarily ignoring or equating any of them. Rather, such a reduction should be effected by the adoption of some sort of superexchange model which will provide additional, physically reasonable relations among them. A simple, unsophisticated model is described and developed in Appendix C. The results given in Table II, where δ denotes the effective anion-anion overlap due to A-site covalency and α is a parameter of the model, show that solutions exist only over a limited range of covalency corresponding to $-0.25<\gamma<0.36$. Furthermore, the derived parameter values fall in rather limited ranges which can be covered by writing $\bar{U}=-0.26\pm0.05$, $V=0.05\pm0.03$, $W=0.075\pm0.035$, $U_2=-0.045\pm0.015$, and $\bar{J}/k=25.4\pm0.4$°K. As pointed out in Appendix C, these solutions

[17] Yung-Li Wang and H. B. Callen, J. Phys. Chem. Solids **25**, 1459 (1964).
[18] S. B. Berger and H. L. Pinch, J. Appl. Phys. **38**, 949 (1967).
[19] R. C. LeCraw, H. Von Phillipsborn, and M. D. Sturge, J. Appl. Phys. **38**, 965 (1976).

even yield plausible values for the exchange contribution from direct overlap of neighboring cations,[20] namely $-0.6<\bar{J}_{\text{direct}}/\bar{J}<-0.17$. Although presented primarily for the purpose of illustration, these results can serve as a zeroth approximation for $ZnCr_2Se_e$. It is hoped that improvement can be achieved both by refinement of the model and by cross reference with analogous results for other chromium-chalcogenide spinels.

APPENDIX A: SUPEREXCHANGE DETAILS

Each exchange constant $\bar{J}_{n\nu,m\mu}$ consists of a sum of superexchange terms, one for each pair of interacting $3d$ wave functions, which will be denoted by curly brackets { }. The contribution from each such term is proportional to the square of the transfer integral involved. These transfer integrals arise from superexchange linkages, defined as sequences of overlapping ionic orbitals beginning and ending with the particular $3d$ wave functions involved in the term, and behave like the products of the orbital overlaps, or like the sums of such products when there are multiple linkages. We shall write the overlap product inside the { }, and enclose the contributions from multiple paths in square brackets [ ].

The cation-anion overlaps involving the three t_{2g} orbitals are all equivalent and can simply be called π, but the overlaps with the two e_g functions are inequivalent and require the notation σ_i with $i=1$, 2. The dominant intermediary anion-anion overlap Δ is illustrated by $\Delta(y_1z_4)$, meaning the overlap between the p_y orbital of anion 1 in Fig. 3 and the p_z orbital of anion 4. With reference to Fig. 3, one can similarly define the lesser overlaps $\Delta_2(y_1y_9)$ and $\Delta'(y_1y_4)$; $\Delta''(x_1x_4)$ is even smaller and $\Delta'''(y_1x_4)$ vanishes. These anion-anion overlaps may be augmented (or diminished, depending upon phases) by covalency with empty A- or B-site cation orbitals, which circumstance will be denoted by a subscript as in $\Delta_A(y_1x_8)$. In the expressions which follow, the symbols σ_i, π, Δ, etc., represent magnitudes; the signs are to be determined from the phase relations among the indicated anion orbitals and the terminating $3d$ functions.

Thus it can be seen from Fig. 3 that

$$\begin{aligned}\bar{J}(B_3\text{-}B_3'') = &\sum_{i,j}\{\sigma_i[\Delta(y_1z_4)+\Delta(z_2y_5)]\sigma_j\}\\ &+\sum_i\{\sigma_i[\Delta'(y_1y_4)+\Delta'(z_2z_5)]\pi\}\\ &+\sum_i\{\pi[\Delta'(z_1z_4)+\Delta'(y_2y_5)]\sigma_i\}\\ &+\{\pi[\Delta_B(z_1y_4)+\Delta_B(y_2z_5)\\ &+\Delta_{2B}(z_1z_5)+\Delta_{2B}(y_2y_4)]\pi\}\\ &+\{\pi\Delta''(x_1x_4)\pi\}+\{\pi\Delta''(x_2x_5)\pi\},\end{aligned}\tag{A1}$$

$$\begin{aligned}\bar{J}(B_3\text{-}B_3') = &\sum_{i,j}\{\sigma_i[\Delta_A(y_1x_8)+\Delta_A(x_3y_7)]\sigma_j\}\\ &+\{\pi[\Delta_A(x_1y_8)+\Delta_A(y_3x_7)+\Delta_2(x_1x_7)\\ &+\Delta_2(y_3y_8)]\pi\}+\sum_i\{\sigma_i[\Delta_A'(y_1y_8)\\ &+\Delta_A'(x_3x_7)]\pi\}+\sum_j\{\pi[\Delta_A'(x_1x_8)\\ &+\Delta_A'(y_3y_7)]\sigma_j\}+\{\pi\Delta_A''(z_1z_8)\pi\}\\ &+\{\pi\Delta_A''(z_3z_7)\pi\}+\sum_i\{\sigma_i\Delta_A'''(y_1z_8)\pi\}\\ &+\sum_i\{\sigma_i\Delta_A'''(x_3z_7)\pi\}+\sum_j\{\pi\Delta_A'''(z_1x_8)\sigma_j\}\\ &+\sum_j\{\pi\Delta_A'''(z_3y_7)\sigma_j\}+\{\pi\Delta_A'''(z_1y_8)\pi\}\\ &+\{\pi\Delta_A'''(x_1z_8)\pi\}+\{\pi\Delta_A'''(y_3z_7)\pi\}\\ &+\{\pi\Delta_A'''(z_3x_7)\pi\},\end{aligned}\tag{A2}$$

$$\begin{aligned}\bar{J}(B_3\text{-}B_4') = &\sum_i\{\sigma_i[\Delta_A(y_1x_8)+\Delta_2(y_1y_9)]\pi\}\\ &+\sum_j\{\pi[\Delta_A(x_1y_8)+\Delta_2(y_3y_8)]\sigma_j\}\\ &+\sum_{i,j}\{\sigma_i\Delta_A'(y_1y_8)\sigma_j\}+\{\pi\Delta_A'(x_1x_8)\pi\}\\ &+\{\pi\Delta_A''(z_1z_8)\pi\}+\sum_i\{\sigma_i\Delta_A'''(y_1z_8)\pi\}\\ &+\sum_j\{\pi\Delta_A'''(z_1y_8)\sigma_j\}+\{\pi\Delta_A'''(x_1z_8)\pi\}\\ &+\{\pi\Delta_A'''(z_1x_8)\pi\},\end{aligned}\tag{A3}$$

$$\begin{aligned}\bar{J}(B_3\text{-}B_1') = &\sum_i\{\sigma_i[\Delta(y_1z_4)+\Delta_A(y_1x_8)]\pi\}\\ &+\sum_j\{\pi[\Delta(x_2y_6)+\Delta_A(z_3y_6)]\sigma_j\}\\ &+\{\pi[\Delta(x_1z_6)+\Delta_A(x_1y_8)+\Delta_A(y_3z_6)\\ &+\Delta_2(y_3y_8)]\pi\}+\{\pi[\Delta_B(z_1y_4)+\Delta_B(z_1x_6)\\ &+\Delta_B(y_2x_6)+\Delta_{2B}(y_2y_4)]\pi\}\\ &+\sum_i\{\sigma_i[\Delta'(y_1y_2)+\Delta_A''(x_3x_6)]\pi\}\\ &+\sum_j\{\pi[\Delta'(y_2y_6)+\Delta_A''(z_1z_8)]\sigma_j\}\\ &+\sum_i\{\sigma_i[\Delta_A'(y_1y_8)+\Delta''(z_2z_6)]\pi\}\\ &+\sum_j\{\pi[\Delta_A'(y_3y_6)+\Delta''(x_1x_4)]\sigma_j\}\\ &+\{\pi[\Delta'(x_1x_6)+\Delta_A'''(y_3x_6)]\pi\}\\ &+\{\pi[\Delta'(x_2x_6)+\Delta_A'''(z_3x_6)]\pi\}\\ &+\{\pi\Delta_A'(x_1x_8)\pi\}+\{\pi\Delta_A'(z_3z_6)\pi\}\\ &+\{\pi\Delta'(z_1z_6)\pi\}+\{\pi\Delta'(z_1z_4)\pi\}\\ &+\sum_{i,j}\{\sigma_i[\Delta_A'''(y_1z_8)+\Delta_A'''(x_3y_6)]\sigma_j\},\end{aligned}\tag{A4}$$

[20] J. B. Goodenough, Phys. Rev. **117**, 1442 (1960).

$$\bar{J}(B_3\text{-}B_3''') = \sum_{i,j}\{\sigma_i[\Delta_2(y_1y_9)+4\Delta_A\Delta-4\Delta_A'\Delta']\sigma_j\}$$
$$+2\{\pi[2\Delta_A\Delta_B-2\Delta_A'\Delta']\pi\}$$
$$+2\sum_i\{\sigma_i[\Delta_A'\Delta_B-2\Delta_A\Delta'+\Delta\Delta_A'+\Delta\Delta_A'''$$
$$-\Delta''\Delta_A''']\pi\}+2\sum_j\{\pi[\Delta_A'\Delta_B-2\Delta_A\Delta'$$
$$+\Delta\Delta_A'+\Delta\Delta_A'''-\Delta''\Delta_A''']\sigma_j\}$$
$$+2\{\pi[2\Delta_B\Delta_A'''-2\Delta'\Delta_A'''-2\Delta''\Delta_A''']\pi\}. \quad (A5)$$

Here it was necessary to include linkages with two anion-anion overlaps because the leading term Δ_2 is small. The overlap product $\Delta_A(y_1x_8)\Delta(x_8y_9)$ was abbreviated as $\Delta_A\Delta$, $\Delta_A'(y_1y_8)\Delta'(y_8y_9)$ as $\Delta_A'\Delta'$, $\Delta_A(x_1y_8)\Delta_B(y_8x_9)$ as $\Delta_A\Delta_B$, etc. The minus signs arise from phase considerations.

APPENDIX B: THE MATRIX L(K)

Given the definitions in Secs. II and III, together with $h'=\frac{1}{2}(\pi h)$, $k'=\frac{1}{2}(\pi k)$, and $l'=\frac{1}{2}(\pi l)$, we can express the elements of the matrix $\mathbf{L}(\mathbf{k})$ as follows:

$$L_{33}(h,k,l)=2U[\cos(2h'+2k')+\cos(2k'+2l')$$
$$+\cos(2l'+2h')]+2U'[\cos(2h'-2k')$$
$$+\cos(2k'-2l')+\cos(2l'-2h')]$$
$$+2U_2[\cos(4h')+\cos(4k')+\cos(4l')]. \quad (B1)$$

The explicit expression for $L_{11}(h,k,l)$ can be obtained from the above equation by everywhere substituting $(-k')$ for k'. Thus we write:

$$L_{11}(h,k,l)=L_{33}(h,\bar{k},l),$$
$$L_{22}(h,k,l)=L_{33}(\bar{h},k,l),$$
$$L_{44}(h,k,l)=L_{33}(h,k,l). \quad (B2)$$

Similarly, for the off-diagonal elements,

$$L_{34}(h,k,l)=2\cos(h'+k')+2V[\cos(3h'-k')$$
$$+\cos(h'-3k')]+2W[\cos(h'-k'+2l')$$
$$+\cos(h'-k'-2l^1)]. \quad (B3)$$

The equation for $L_{12}(h,k,l)$ can be obtained from this expression by everywhere substituting $(-k')$ for k'. Consequently, we write

$$L_{12}(h,k,l)=L_{34}(h,\bar{k},l),$$
$$L_{13}(h,k,l)=L_{34}(l,h,k),$$
$$L_{14}(h,k,l)=L_{34}(k,\bar{l},h),$$
$$L_{23}(h,k,l)=L_{34}(k,l,h),$$
$$L_{24}(h,k,l)=L_{34}(l,\bar{h},k). \quad (B4)$$

Finally,

$$L_{\nu\mu}(h,k,l)=L_{\mu\nu}(h,k,l). \quad (B5)$$

APPENDIX C: SIMPLIFIED SUPEREXCHANGE MODEL

The superexchange terms $\sum_i\{\sigma_i\Delta\pi\}$ appearing in Appendix A can be expressed as $\{\sigma_{zz}\Delta\pi\}$, where σ_{zz} represents the overlap of a cation d_z^2 orbital and a coaxial anion p_z, and for the case of octahedral Cr^{3+}, a positive number α can be defined such that $\{\sigma_{zz}\Delta\pi\}=-\alpha\{\pi\Delta\pi\}$. For convenience, let us arbitrarily set $\{\sigma_{zz}\Delta\sigma_{zz}\}=-\alpha\{\sigma_{zz}\Delta\pi\}$. The relative strengths of the other σ overlaps of the d_z^2 and $d_{x^2-y^2}$ orbitals are rigorously $\sigma_{zx}=\sigma_{zy}=-\frac{1}{2}\sigma_{zz}$, $\sigma_{xz}=0$, and $\sigma_{xx}=-\sigma_{xy}=\frac{1}{2}\sqrt{3}\sigma_{zz}$, where the first subscript denotes which e_g orbital and the second denotes the bond axis. Then, for example, the first term in Eq. (A1) becomes $0.625\{\sigma_{zz}[2\Delta]\sigma_{zz}\}=2.5\{\sigma_{zz}\Delta\sigma_{zz}\}=2.5\alpha^2\{\pi\Delta\pi\}$, where we recall that the superexchange behaves like the square of the overlaps indicated in the brackets.

Let us approximate $\Delta_2=\Delta'=\Delta''=\Delta'''=0$, and let δ represent the effective anion-anion overlap resulting from mutual covalence with an empty s orbital of the diamagnetic A-site cation. Then $\Delta_A'=\Delta_A''=\Delta_A'''=\delta$ and $\Delta_A=\Delta+\delta$. Covalency with the empty e_g orbitals of the Cr^{3+} B-site ions is relatively ineffective in Eqs. (A1) and (A4), since its contributions to Δ_{2B} and Δ_B almost cancel. Consequently very little error is introduced in writing $2\Delta_B+2\Delta_{2B}\cong 2\Delta$ and $3\Delta_B+\Delta_{2B}\cong 3\Delta$.

The parameters $\bar{U}$, γ, V, and W can all be expressed in terms of the new variables $\{\pi\Delta\pi\}$, α, and δ/Δ. For most choices of α and δ/Δ, the resulting solution of Eq. (25) does not fall in the stability region of Fig. 6. Table II covers the entire range of stable solutions. We see that δ/Δ must lie between 0.3 and -0.29, that α must lie between 3 and 7, and that the values of $\bar{U}$, V, W, and U_2 are narrowly circumscribed.

The parameter U_2 can also be expressed in terms of $\{\pi\Delta\pi\}$, α, and δ/Δ if we introduce a new variable β to represent explicitly the effect of additional anion-anion overlaps on the superexchange, that is, $\{\pi\Delta\Delta\pi\}=\beta\{\pi\Delta\pi\}=\beta^2\{\pi\pi\}$. Then the values in Table II yield $0.020<\beta<0.033$. But α and $\{\pi\pi\}=\{\pi\Delta\pi\}/\beta$ determine the nearest-neighbor superexchange, namely

$$\bar{J}_{\text{exch}}=\sum_i\{\sigma_i\pi\}+\sum_j\{\pi\sigma_j\}+2\{\pi\pi\},$$

and

$$\bar{J}=\bar{J}_{\text{exch}}+\bar{J}_{\text{direct}},$$

where $\bar{J}_{\text{direct}}$ is the antiferromagnetic exchange contribution from direct overlap of the cation t_{2g} orbitals.[20] The values for $\bar{J}_{\text{direct}}/\bar{J}=1-\bar{J}_{\text{exch}}/\bar{J}$ implicit in Table II run from -0.17 to -0.6; they increase negatively with increasing α and increasing δ/Δ. Since these values do not seem physically unreasonable, we conclude that the solutions shown in Table II are self-consistent.